AD-A120 339 TEXAS UNIV AT AUSTIN APPLIED RESEARCH LABS F/G 20/1
PRELIMINARY RESULTS OF AN EVALUATION OF THE EFFICIENCY OF VLF S--ETC(U)
AUG 82 P J VIDMAR N00014-81-K-0353
UNCLASSIFIED ARL-TR-82-36 NL

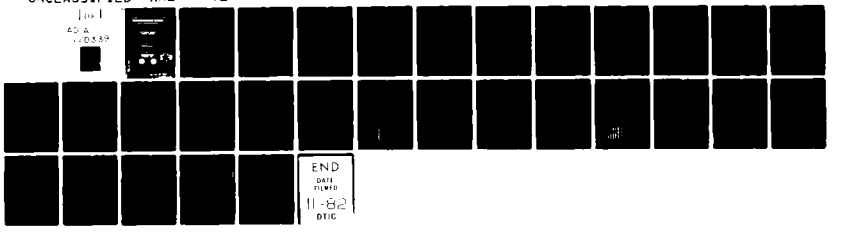

END
DATE FILMED
11-82
DTIC

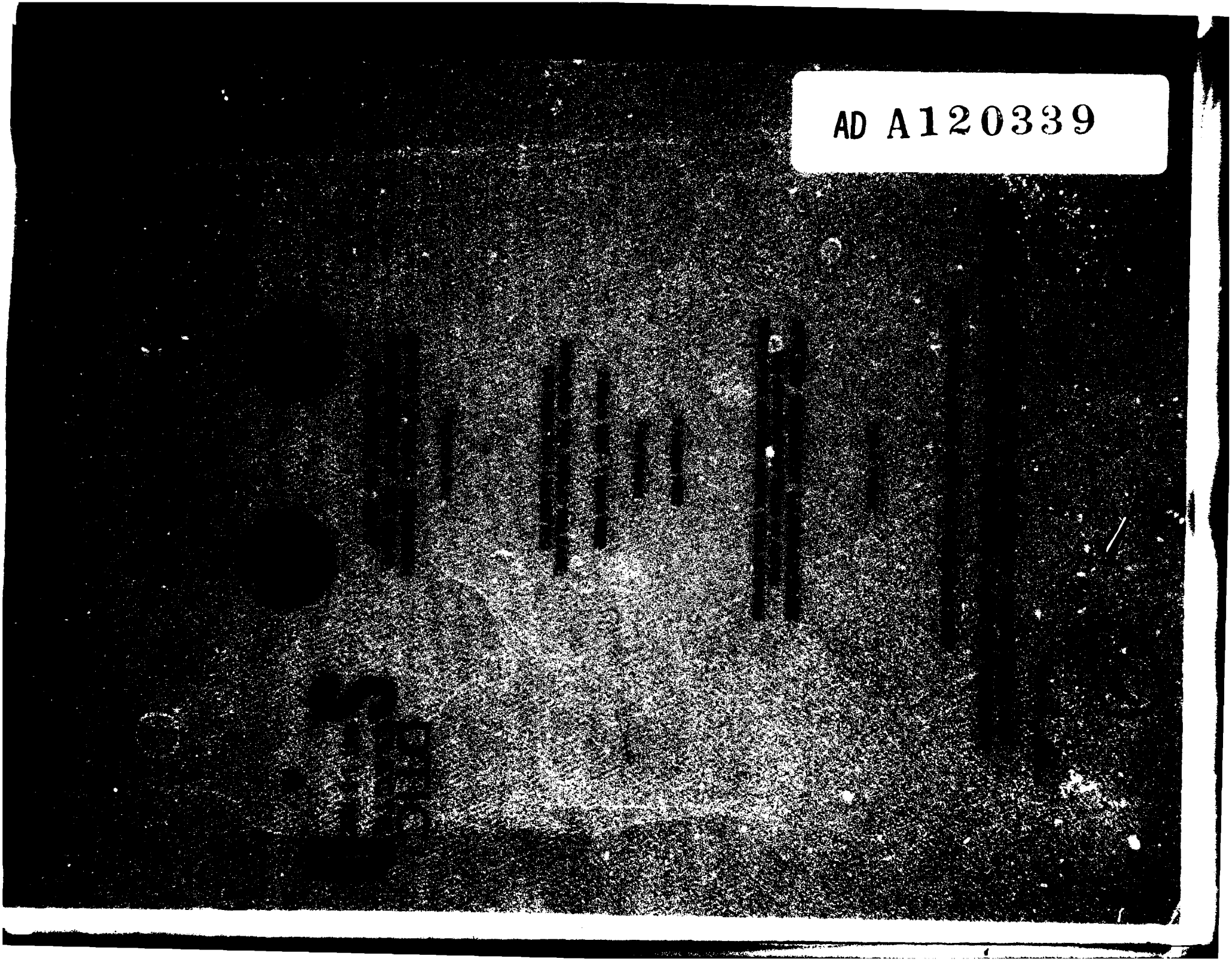

UNCLASSIFIED

SECURITY CLASSIFICATION OF THIS PAGE (When Data Entered)

REPORT DOCUMENTATION PAGE		READ INSTRUCTIONS BEFORE COMPLETING FORM
1. REPORT NUMBER	2. GOVT ACCESSION NO. AD-A120 339	3. RECIPIENT'S CATALOG NUMBER
4. TITLE (and Subtitle) PRELIMINARY RESULTS OF AN EVALUATION OF THE EFFICIENCY OF VLF SEISMIC PROPAGATION IN A CONTINENTAL SLOPE ENVIRONMENT		5. TYPE OF REPORT & PERIOD COVERED Final Report 2 March 1981 - 1 March 1982
		6. PERFORMING ORG. REPORT NUMBER ARL-TR-82-36
7. AUTHOR(s) Paul J. Vidmar		8. CONTRACT OR GRANT NUMBER(s) N00014-81-K-0353
9. PERFORMING ORGANIZATION NAME AND ADDRESS Applied Research Laboratories The University of Texas at Austin Austin, TX 78712-8029		10. PROGRAM ELEMENT, PROJECT, TASK AREA & WORK UNIT NUMBERS
11. CONTROLLING OFFICE NAME AND ADDRESS Office of Naval Research Department of the Navy Arlington, VA 22217		12. REPORT DATE 6 August 1982
		13. NUMBER OF PAGES 31
14. MONITORING AGENCY NAME & ADDRESS(if different from Controlling Office)		15. SECURITY CLASS. (of this report) UNCLASSIFIED
		15a. DECLASSIFICATION/DOWNGRADING SCHEDULE

16. DISTRIBUTION STATEMENT (of this Report)

Approved for public release; distribution unlimited.

17. DISTRIBUTION STATEMENT (of the abstract entered in Block 20, if different from Report)

18. SUPPLEMENTARY NOTES

19. KEY WORDS (Continue on reverse side if necessary and identify by block number)

underwater acoustics
low frequency
subbottom propagation
continental slope
frequency band analysis

20. ABSTRACT (Continue on reverse side if necessary and identify by block number)

Data collected in a continental slope geometry were used to investigate the efficiency of low frequency bottom penetrating propagation. Preliminary ray trace and bottom loss modeling were used to estimate the duration of the water-borne component of shot data and to identify shots containing potential sediment penetrating arrivals. Frequency band analysis of the time series of a shot was used to confirm the identification of a subbottom penetrating arrival on the basis of its loss of high frequency energy due to absorption within the subbottom. Propagation loss, estimated using the theoretical source spectrum,

DD FORM 1 JAN 73 1473 EDITION OF 1 NOV 65 IS OBSOLETE

UNCLASSIFIED

SECURITY CLASSIFICATION OF THIS PAGE (When Data Entered)

20. (Cont'd)

was used to compare low frequency propagation along a subbottom path to high frequency propagation along a waterborne path. This comparison showed that for a source in deep water and a bottomed receiver on the continental slope, the efficiency of 35 Hz bottom penetrating propagation is comparable to, if not better than, propagation along a waterborne path over the 35-1000 Hz frequency range studied.

TABLE OF CONTENTS

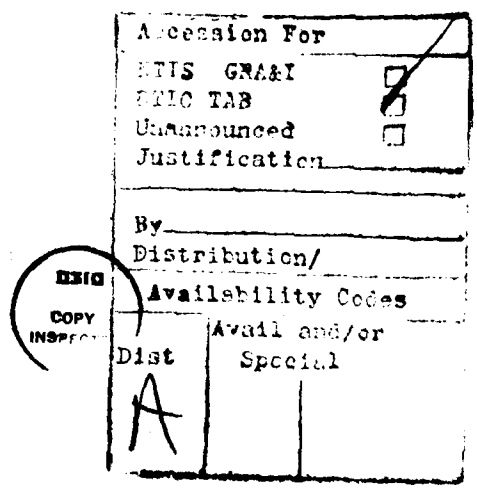

LIST OF FIGURES

I. INTRODUCTION

Surveillance and tactical antisubmarine warfare (ASW) acoustic systems currently rely on predominantly waterborne propagation paths. However, for a wide variety of source-receiver geometries, acoustic frequencies, sound speed profiles, and water depths, sound propagation in the ocean can be heavily influenced by the ocean bottom. At this time, some currently operating and projected systems make use of bottom interacting energy or have sensors purposely located near the ocean bottom. With few exceptions, the major role of acoustic bottom interaction has been to place limitations on the frequencies and distances over which such systems will operate reliably.

The question naturally arises as to whether the bottom penetrating energy can be directly exploited for ASW applications. This question is particularly relevant for applications in areas where bottom interaction is an important factor influencing acoustic propagation. Some examples are shallow water propagation, deep-to-shallow water transitions, and propagation to slope mounted sensors. The answer may very well be in the affirmative at very low frequencies (VLF) where the propagation via bottom penetrating (seismic) paths becomes favorable.

This report summarizes work carried out by Applied Research Laboratories, The University of Texas at Austin (ARL:UT), to investigate the efficiency of very low frequency (VLF) propagation along subbottom paths in the continental slope environment. The goal of this work was not to carry out extensive data analysis and interpretation, but rather to compare sediment penetrating propagation at low frequencies to the primarily waterborne (including sediment reflected) propagation at the higher frequencies. Such a comparison is necessary to evaluate potential advantages of VLF propagation in the context of ASW

applications. Other topics which have bearing on this evaluation, such as the advantages of using geophones rather than hydrophones as VLF sensors and potential signal-to-noise advantages, were not within the scope of this work.

The remainder of this report is organized as follows. Section II discusses relevant aspects of the experimental geometry and data, including analog-to-digital (A/D) conversion, data quality, and calibration. Section III describes the analysis and interpretation of sample data and the evaluation of the efficiency of VLF seismic propagation. Section IV summarizes the investigation.

II. EXPERIMENTAL GEOMETRY AND DATA

A. Exercise Description

Figure 1 shows the exercise area off the coasts of Nova Scotia and Newfoundland. The locations of the hydrophones used to collect data are shown along with the source track. The track is roughly along the bathymetry gradient.

The hydrophone locations and bathymetry along the source track are shown in more detail in Fig. 2. The range is relative to the beginning of the source track which extends out to 66.3 km. Hydrophones 4, 5, 6, and 7 are on the ocean bottom, while hydrophones 1, 2, and 3 are buoyed. Signals collected using these hydrophones comprised the data set available for analysis by ARL:UT.

Three traverses were made of the source track in Fig. 1, each using a different acoustic source. The first, from north to south, used standard 1.8 lb (0.82 kg) TNT Mk 61 SUS charges fired at a depth of 18 m. The second run, from south to north, used a 31 Hz cw signal as the acoustic source. The third run used small 1.1 oz charges fired alternately at 18 m and 91 m. An unscheduled seismic reflection study using air gun sources was also conducted during the exercise along a generally east-west line between zero range and hydrophone 7 in Fig. 2. Additional information available included navigation, hydrophone sensitivity, changes in amplifier gain during the exercise, and measured sound velocity profiles at three locations near the source track (start, hydrophone 6, and end). For the studies reported here, only the shot data were used since they provide timing information needed to identify arrivals traveling along different propagation paths. Such information is absent in cw data.

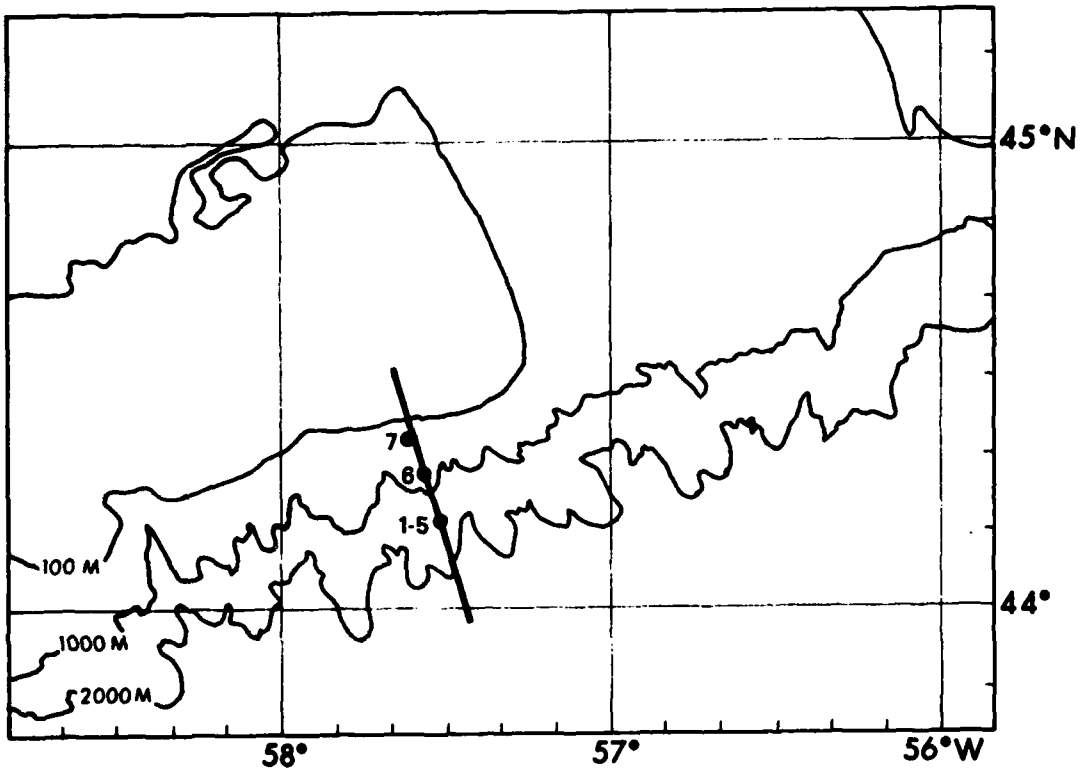

FIGURE 1
EXERCISE AREA

ARL:UT
AS-82-1192
PJV - GA
8 - 4 - 82

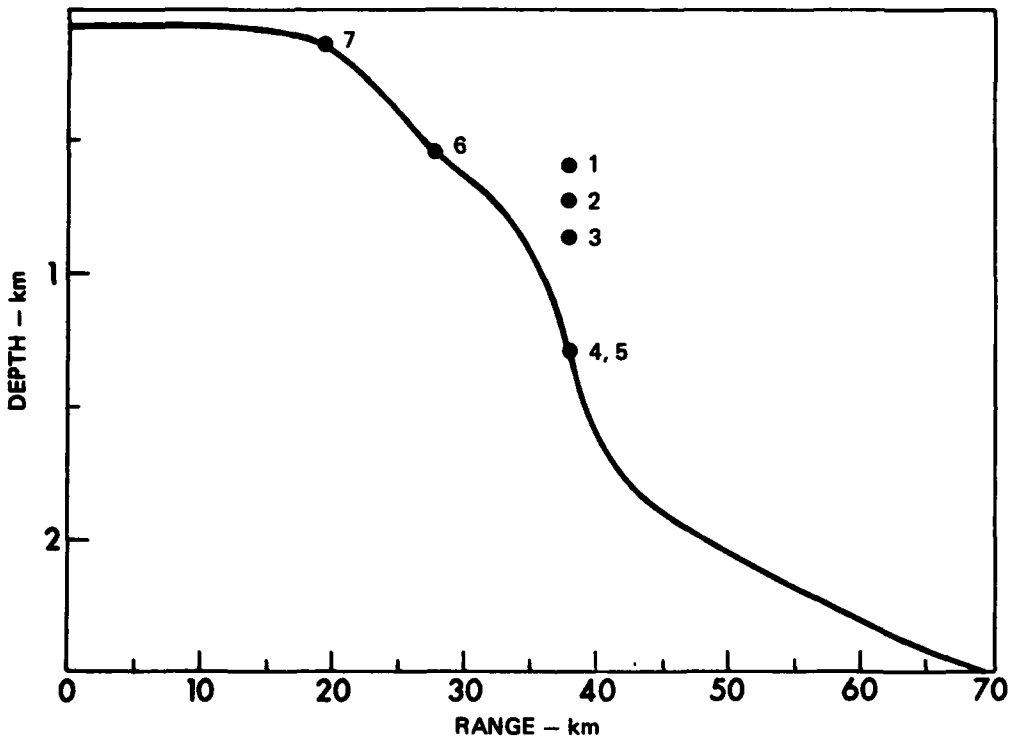

FIGURE 2
BATHYMETRY AND HYDROPHONE LOCATIONS ALONG THE SOURCE TRACK

ARL:UT
AS-82-1193
PJV - GA
8 - 4 - 82

Figure 3 is a schematic of the geoacoustic structure along the source track. The area is a highly complex geological environment.[1] The first 1.6-1.7 km of sediment consists of unconsolidated to semiconsolidated terrigeneous sediments containing significant glacial erratics. The layers below consist of highly consolidated carbonate (reef), shale, and salt. The basement includes both oceanic and continental crust. The layer thicknesses are not constant but vary according to their position along the exercise track. The sound speed estimates were determined from published average values[2] for the area.

B. Data Reduction and Quality Assessment

Data from the two shot runs and the cw tow were first subjected to an analog data quality assessment. Each channel was analyzed to verify the presence of data, timing information, and calibration tones. Sections of data with missing time code were identified. The data tapes were found to contain useful data from part of the large shot run, all of the small shot run, and all of the cw tow. The data from the large shots were determined to be severely clipped. The analog shot data were digitized with a 2500 Hz sampling rate which then allowed data to be analyzed up to 1250 Hz.

Calibration tones on the tapes and hydrophone sensitivity data were combined to produce the system transfer function. Six calibration tones from 20 to 500 Hz were recorded on the original tapes. Figure 4 shows the transfer function for the combined recording and reproduction system of tape drives and amplifiers obtained from the calibration tones. This transfer function is generally independent of frequency over a wide band and was extrapolated both up and down in frequency. Figure 4 also shows the reported hydrophone sensitivity. Experience shows that these curves may be accurately extrapolated to higher frequencies but not to lower. The final curve in Fig. 4 is the composite transfer function for the hydrophone/record-playback system. For use in our data analysis, this transfer function was used from 10 to 400 Hz and was extrapolated from 400 to 1250 Hz, assuming it to be independent of frequency.

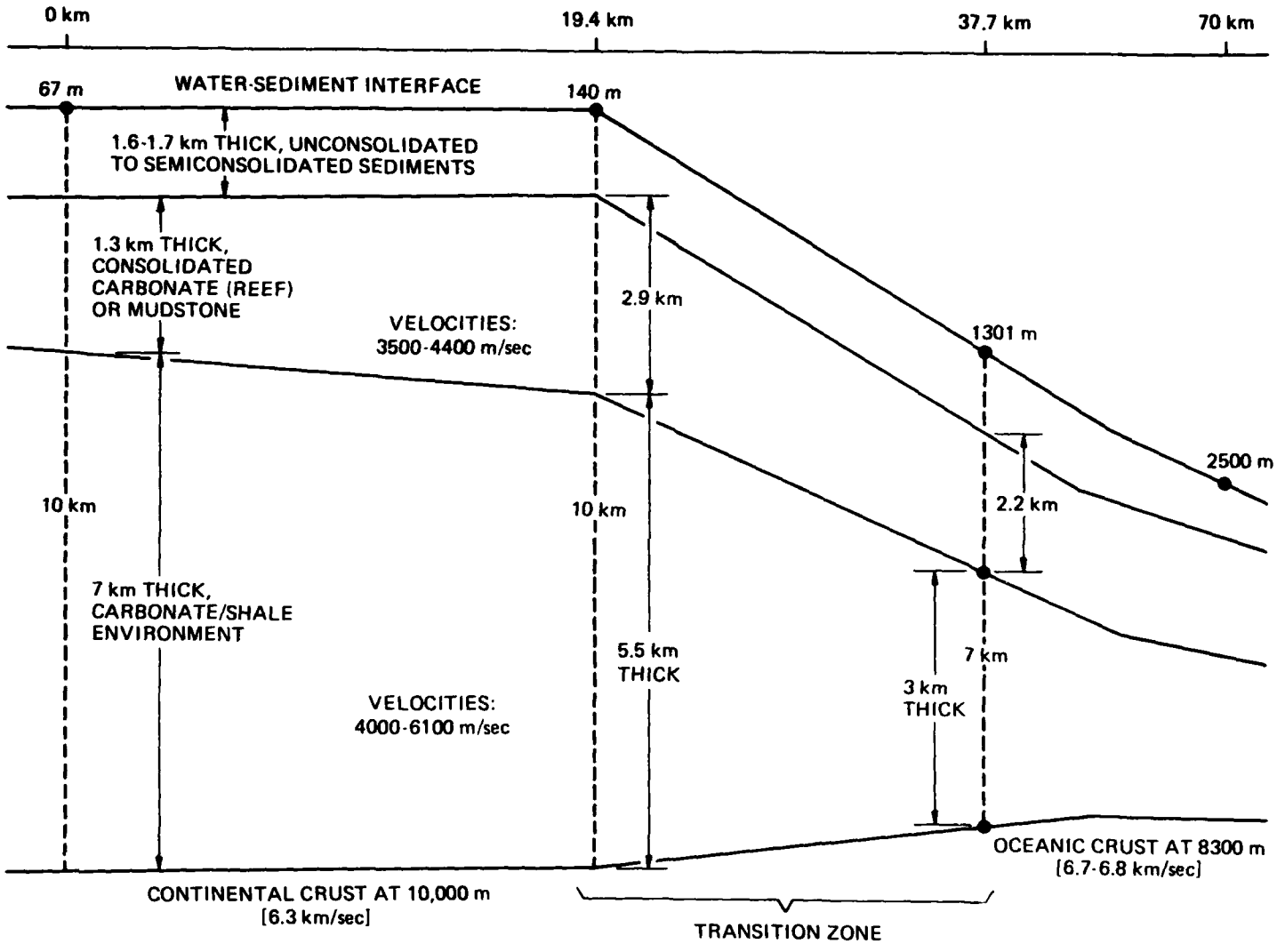

FIGURE 3
GEOLOGICAL STRUCTURE OF THE EXERCISE AREA

ARL:UT
AS-81-1037
MJD-GA
8-17-81
REV 8-4-82

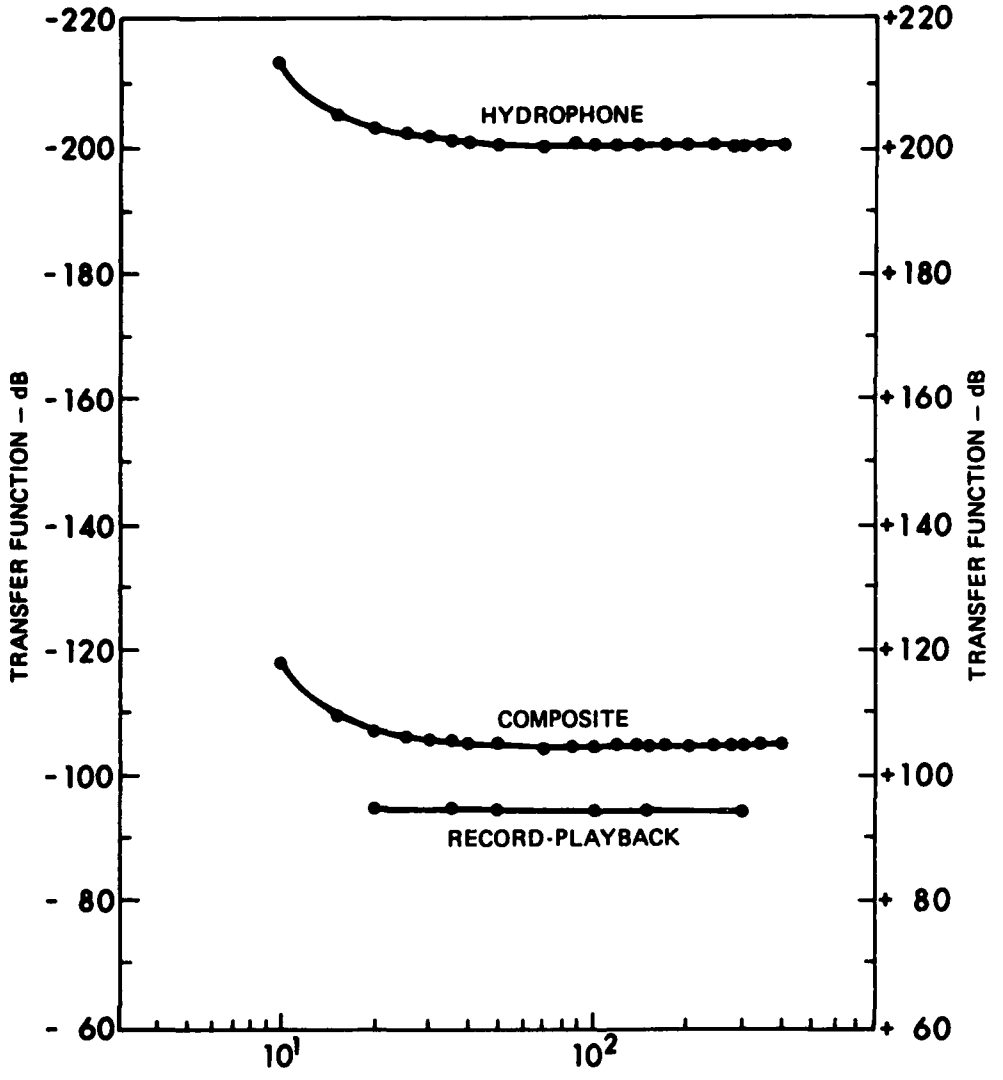

FIGURE 4
TRANSFER FUNCTIONS FOR HYDROPHONE 4

HYDROPHONE TRANSFER FUNCTION (V/μPa) AND RECORD-PLAYBACK TRANSFER FUNCTION (V/DIGITIZED NUMERIC VALUE) USE THE LEFT SCALE. THE COMPOSITE TRANSFER FUNCTION (μPa/DIGITIZED NUMERIC VALUE) USES THE RIGHT SCALE.

ARL:UT
AS-82-1194
PJV - GA
8 - 4 - 82

The location of hydrophone 7 at the top of the slope in Fig. 2 is best suited to study coupling to subbottom paths from sources in deep water. This location provides the maximum opportunity for energy from deep water sources to encounter the slope and to propagate through the subbottom to the receiver. To assess the quality of data collected on this hydrophone, a sample large shot and small shot were analyzed.

Anomalous features, including almost constant level and harmonically related peaks, in the signal spectra of both large and small shots suggested that shot data collected by hydrophone 7 were not usable. On the basis of laboratory tests of a record-playback system, the source of the anomalies was identified as overdeviation effects occurring when the frequency modulation system used to record the original data on magnetic tape was driven outside the acceptable frequency range. Hence, data from hydrophone 7 were found to be unacceptable for further analysis.

Under the assumption that signal levels would be lower in deeper water, small shot data from hydrophone 4 at a 1300 m depth were examined next for data quality. The signal spectra were qualitatively different from those seen in data from hydrophone 7. The spectra decreases with frequency as is typical of shot data. The time series are also qualitatively different. Multiple arrivals were identified and compared to the case with data from hydrophone 7 where only one arrival could be identified. Data from hydrophone 4 were used in the analysis described below.

In summary, shot data were digitized and system calibration determined. Both large and small shot data from hydrophone 7, located at the top of the slope, were overdeviated and not acceptable for our analysis. Small shot data from hydrophone 4, the deepest location, were found to be acceptable for further analysis.

III. DATA ANALYSIS AND INTERPRETATION

The objective of this analysis was to evaluate the efficiency of low frequency, bottom penetrating propagation in a continental slope geometry. The procedure followed to achieve this objective had several components. Modeled propagation in the water column was compared with observed shot arrival structure to select a shot having clearly identifiable, non-waterborne arrivals and to identify a candidate subbottom propagating arrival. This shot was analyzed in detail. The received time series was displayed in 50 Hz passbands with center frequencies from 35 to 1000 Hz. The observed lack of high frequency content in the candidate subbottom arrival was consistent with absorption within the subbottom, strengthening its identification as a bottom penetrating arrival. Propagation loss as a function of frequency at a fixed range for this arrival and for the first arrivals were quantitatively compared to determine the efficiency of propagation along the subbottom path. This comparison showed that propagation at 35 Hz along the subbottom penetrating path is as efficient as propagation from 35 to 1000 Hz along the first arrival path.

A. Shot Selection

To select shots for detailed analysis, a combination of propagation modeling and observation of shot structure was used. The goal of the propagation modeling was to determine the arrival structure of energy propagating within the water column without penetrating the ocean bottom. With this information, shot arrival structures were examined and several candidate shots were found to have arrivals clearly not anticipated from the modeling of waterborne propagation. One of these shots was chosen for detailed analysis.

The propagation modeling used the ARL:UT ray model, MEDUSA,[3] to determine eigenrays for the range varying water depth and sound velocity environment of the experimental area. MEDUSA provided waterborne eigenrays, including those reflected from the sediment surface, intensities, ranges at which bottom reflection occurred, bottom reflection angles, arrival times, and ray angles at the source.

The water-sediment interface reflection coefficient was examined to provide an estimate of the reflection loss for bottom reflected rays. Parameters estimated from published data for the area[2] and empirical relations among sedimentary parameters[4] indicate that rays reflected at grazing angles greater than 10^{o} suffer a reflection loss of about 15 dB. Those reflected below 10^{o} are almost perfectly reflected.

The propagation modeling showed that for the longer downslope ranges near the end of the source track, the direct waterborne arrival ceases to exist and all eigenrays reflect at least once from the slope before reaching hydrophone 4. The first arrival has a bottom grazing angle of about 8^{o} while the two-, three-, and four-bounce arrivals have grazing angles between 15^{o} and 40^{o}. Spreading loss was about the same for all four arrivals. Travel times for the two-, three-, and four-bounce arrivals relative to the one bounce-arrival were typically 0.5, 1.5, and 2.6 sec, respectively.

Combining the propagation modeling results with the bottom reflection loss suggests that, relative to the one-bounce arrival, the three- and four-bounce waterborne arrivals will suffer an additional 30-45 dB reflection loss, and hence will not have significant amplitudes. The expected waterborne signal duration is then about 0.5-1.5 sec at most, if the three-bounce arrival is included. Thus, any energetic arrival occurring after about 1 sec from the onset is a candidate for a sediment penetrating arrival.

Figure 5 shows a rectified and averaged envelope of the shot chosen for analysis. It was produced by an 18 m deep small shot received on

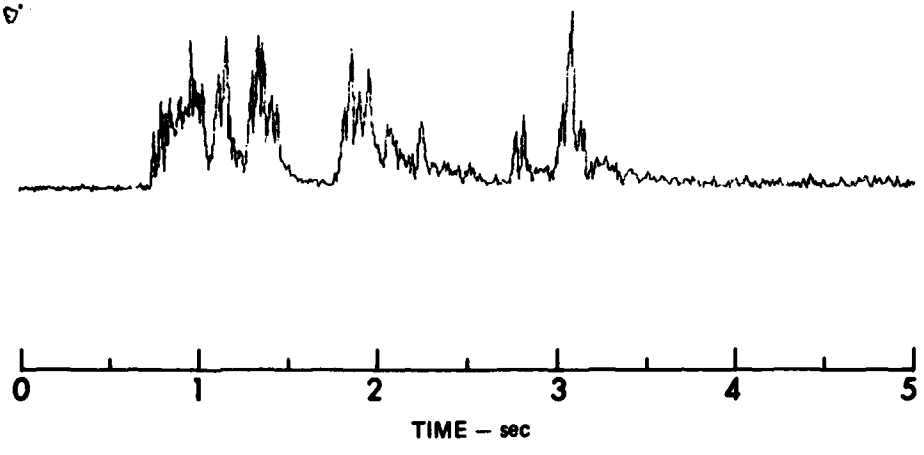

FIGURE 5
RECTIFIED SMALL SHOT WAVEFORM
RECEIVED ON HYDROPHONE 4

ARL:UT
AS-82-1195
PJV - GA
8 - 4 - 82

hydrophone 4. Navigation logs give the source range as 26.4 km downslope from hydrophone 4. Energy arriving in distinct bundles can clearly be distinguished. On the basis of the above discussion, the two late arrivals occurring between 2 and 2.5 sec after the onset of the signal (between 2.75 and 3.25 sec in Fig. 5) are clearly candidates for sediment penetrating arrivals. Several other arrivals are also candidates but our attention will be focused on the very large arrival occurring at about 3.0 sec in Fig. 5.

B. Detailed Shot Analysis

Figure 6 shows the received time series corresponding to the signal envelope in Fig. 5. The display origin is about 10 msec before the onset of the first arrival. The time series clearly shows the different frequency content of the waterborne first arrival (W) and the candidate subbottom penetrating arrival (S) at about 2.3 sec. The lack of high frequency content in S strengthens its identification as a sediment penetrating arrival.

Figure 7 shows the frequency spectra of W and S along with the noise spectrum taken in the time interval between this shot and the preceding shot. Both arrivals have signal excess of at least 20 dB at low frequencies. Arrival W maintains this signal excess out to 1250 Hz, while arrival S decays to about 3 dB at higher frequencies. The shapes of the two spectra are also different. Arrival W has a rather gentle decrease in power with increasing frequency. It also has a region below 100 Hz where signal strength falls off rapidly with decreasing frequency. The nature of this decrease in low frequency content is not yet understood and will be commented on again when propagation loss is examined. The arrival S has a totally different spectrum. The signal energy peaks at low frequencies and decreases at higher frequencies much more rapidly than that of arrival W.

The source spectrum in 50 Hz bands for a 1.1 oz shot detonated at an 18 m depth is shown in Fig. 8. This spectrum was computed by Fourier transforming the time series, which was generated according to published theoretical work[5] giving the dependence of the pressure waveform on shot

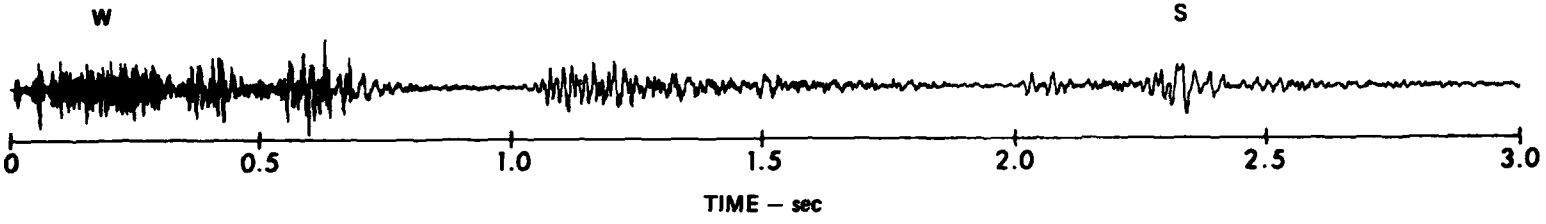

FIGURE 6
RECEIVED TIME SERIES

ARL:UT
AS-82-1198
PJV-GA
8-4-82

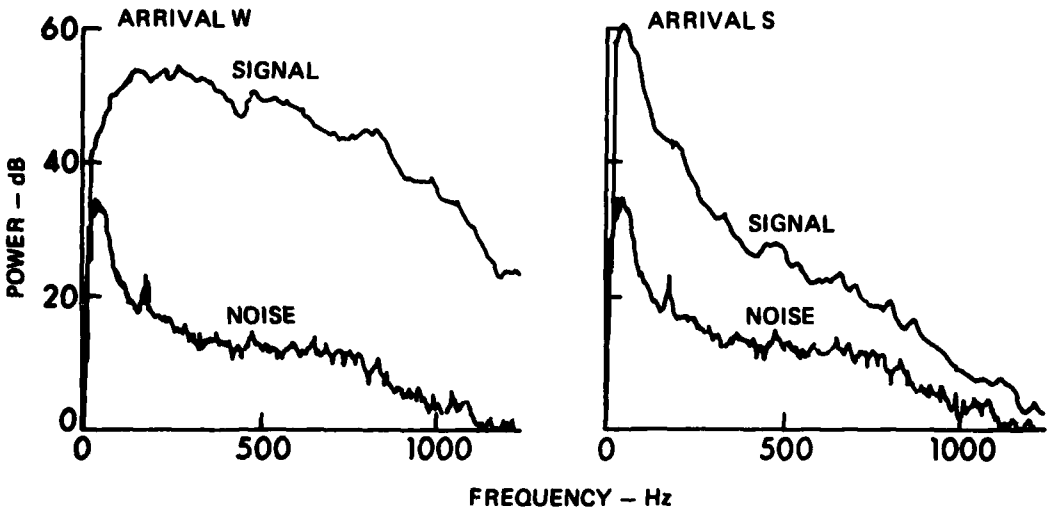

FIGURE 7
SIGNAL AND NOISE SPECTRA FOR ARRIVALS W AND S

ARL:UT
AS-82-1197
PJV - GA
8 - 4 - 82

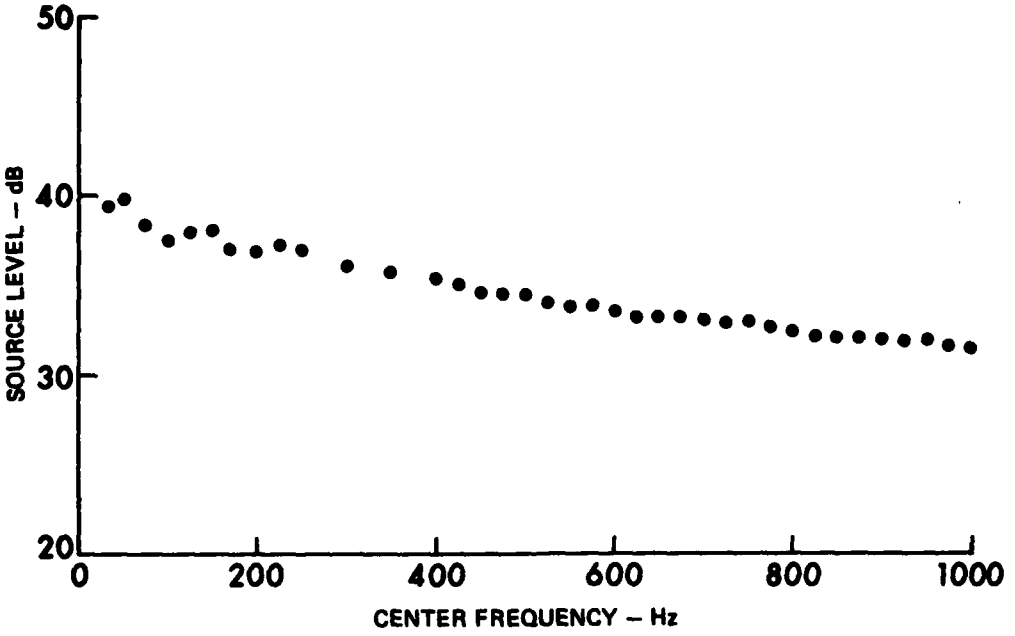

FIGURE 8
SOURCE SPECTRUM IN 50 Hz BANDS

ARL:UT
AS-82-1198
PJV - GA
8 - 4 - 82

weight and detonation depth. There is a change of about 9 dB in source strength over the 10-1250 Hz range used in this study. The bubble pulse frequency is about 24 Hz.

Figure 9 displays the time series in ten 50 Hz frequency bands from 35 to 1000 Hz. These time series have been calibrated using the system transfer function and normalized to remove the dependence on the 1.1 oz shot source level. The disappearance of arrival S above 200 Hz is consistent with absorption along a bottom penetrating path, further strengthening the identification of S as a sediment penetrating arrival. Several other arrivals also appear to be bottom penetrating, but our attention will be focused on S, which is particularly strong. Arrival W has the high frequency content expected in a waterborne arrival. This approach, of identifying sediment reflected and subbottom penetrating arrivals on the basis of its lack of high frequency content, follows the procedure of Christensen et al.[6]

To evaluate the efficiency of propagation along the bottom penetrating path of arrival S, propagation loss will be compared to that of arrival W, the reference waterborne path. Figure 10 compares propagation loss for arrivals W and S. Two features are noteworthy. First is the different frequency dependence of propagation loss for the two arrivals. The relatively constant propagation loss for arrival W from about 100 Hz to 800 Hz suggests a primarily waterborne propagation path for which there is little absorption. The generally increasing loss with frequency seen for arrival S suggests the frequency dependent absorption occurring in sediments.[4] The second feature is that the propagation loss for the bottom penetrating path below 70 Hz is equal to or better than that of the waterborne path at any frequency. Low frequency subbottom propagation is, in this example, as efficient as, or slightly more efficient than, high frequency waterborne propagation.

The high loss below 100 Hz for arrival W is not understood at this time. The most likely explanation is a destructive interference between the different ray paths making up W. The location of the source near the

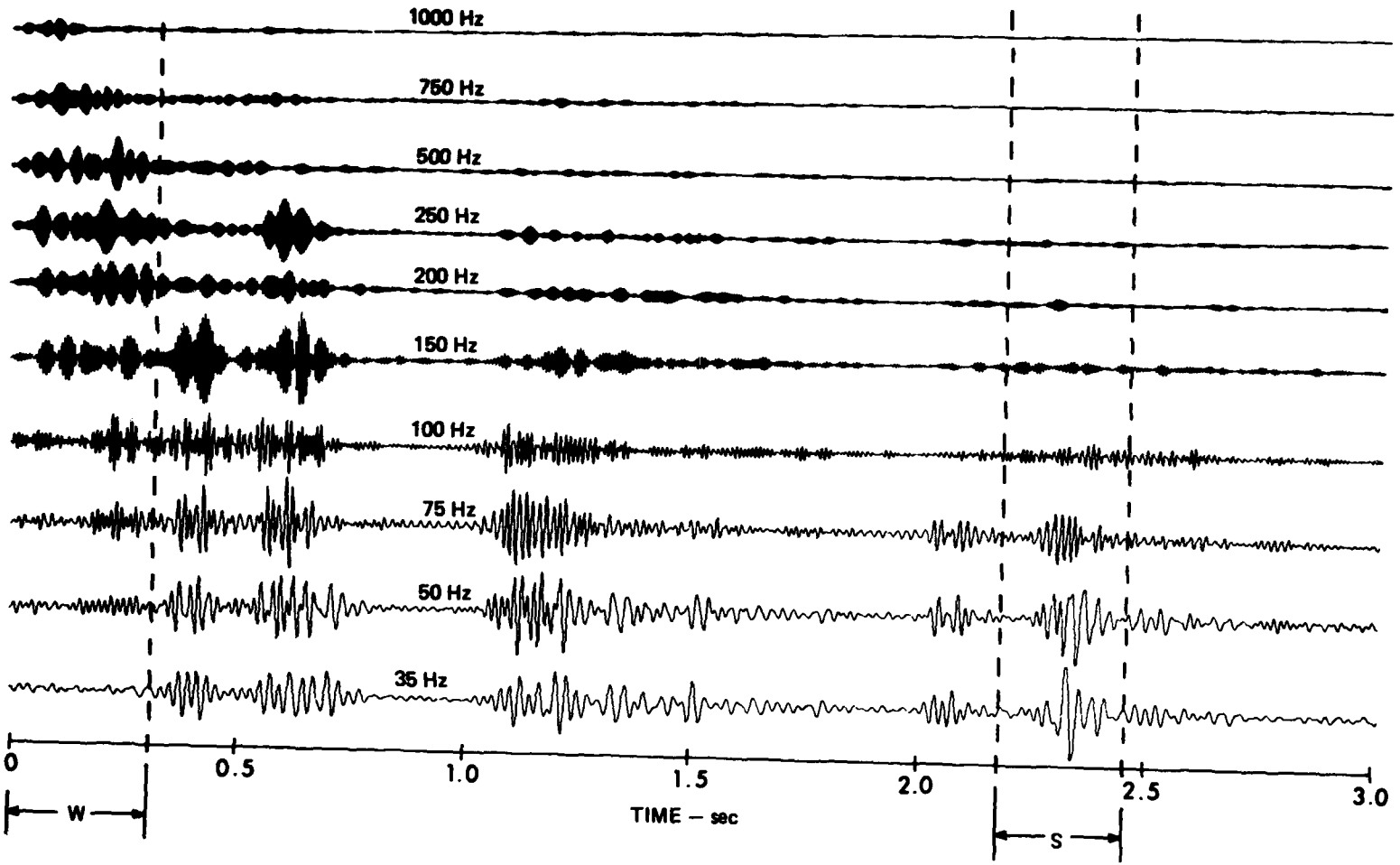

FIGURE 9
TIME SERIES IN 50 Hz BANDS

ARL:UT
AS-82-1199
PJV-GA
8-4-82

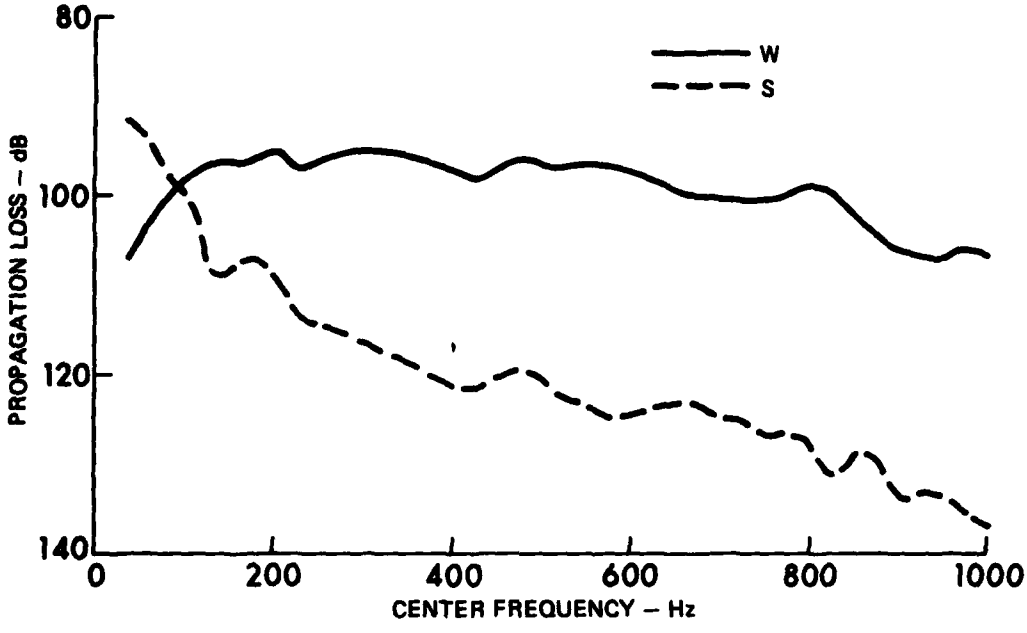

FIGURE 10
PROPAGATION LOSS FOR ARRIVALS W AND S
AS A FUNCTION OF FREQUENCY

ARL:UT
AS-82-1200
PJV - GA
8 - 4 - 82

surface would contribute to this effect, but estimates of this effect using travel time from our preliminary modeling account for only about half of the 10 dB increase in propagation loss at 35 Hz. More detailed modeling of propagation, including the effects of the bottom reflection phase shift, source spectrum, and possible interference from bottom penetrating eigenrays with travel times near that of W, may be needed to resolve this question.

In summary, a frequency band analysis procedure was applied to sample SUS data from a continental slope environment. A candidate sediment penetrating path was first identified on the basis of travel time considerations. Its identification was then strengthened by observing the time series from a number of 50 Hz bands from 35 to 1000 Hz. Comparison of propagation loss for this path and a waterborne path showed that propagation from an 18 m source along the subbottom path at 35 Hz compares favorably to primarily waterborne propagation over the entire frequency range studied, 35 to 1000 Hz.

IV. SUMMARY

SUS data were used to evaluate the efficiency of low frequency, bottom penetrating propagation from a near-surface source in deep water to a bottomed hydrophone in shallower water on the continental slope. A comparison of modeled and measured propagation times was used to select for analysis a shot having a candidate subbottom arrival. An analysis of time series of this shot in a number of 50 Hz frequency bands verified the identification of the bottom penetrating arrival. Propagation loss for the subbottom arrival and a reference waterborne arrival were compared as a function of frequency at a fixed range. For the shot analyzed, ray modeling showed that the direct arrival was absent and that the reference arrival suffered one bottom bounce. Energy contained in the sediment penetrating arrival at 35 Hz was found to be comparable to that contained in the reference waterborne arrival at higher frequencies, i.e., the low frequency sediment-penetrating path was at least as efficient as the waterborne path over a wide frequency range. Further work is needed to identify the particular sediment penetrating path seen in the data.

ACKNOWLEDGMENTS

This work would not have been possible without the cooperation and assistance of Mr. Ron Scudder of Western Electric Company, who has archived the data and provided much background information. Many individuals at ARL:UT provided their expertise and talents. Of particular note are the efforts of N. Bedford in the data reduction, T. DeMary in working out the calibrations, and J. Lynch in overseeing the analog-to-digital conversion process and initial data analysis. Thanks are also due to J. M. Daniels for working out the geoacoustic analysis, and to K. E. Hawker and S. K. Mitchell for many suggestions and fruitful discussions.

REFERENCES

1. C. E. Keen and A. Cordsen, "Crystal Structure and Seismic Stratigraphy of the Rifted Continental Margin off Eastern Canada: Ocean Bottom Seismic Refraction Results off Nova Scotia", submitted for publication in C.J.E.S. (1981).

2. T. M. Brocher, B. T. Iwatalee, J. F. Gettrust, G. E. Sutton, and L. N. Frazer, "Comparison of the S/N Ratios of Low-Frequency Hydrophones and Geophones as a Function of Ocean Depth", Bull. Seis. Soc. Am. 71, 1649-1659 (1981).

3. T. L. Foreman, "The ARL:UT Range Dependent Ray Model, MEDUSA", Applied Research Laboratories Technical Report, Applied Research Laboratories, The University of Texas at Austin, in preparation.

4. E. L. Hamilton, "Geoacoustic Modeling of the Sea Floor", J. Acoust. Soc. Am. 68, 1313-1340 (1980).

5. J. Wakely, Jr., "Coherent Ray Tracing-Measured and Predicted Shallow Water Frequency Spectrum," J. Acoust. Soc. Am. 63, 1820-1823 (1978).

6. R. E. Christensen, J. A. Frank, and W. H. Geddes, "Low-Frequency Propagation via Shallow Refracted Paths through Deep Ocean Sediments", J. Acoust. Soc. Am. 57, 1421-1426 (1975).

6 August 1982

DISTRIBUTION LIST FOR
ARL-TR-82-36
FINAL REPORT UNDER CONTRACT N00014-81-K-0353
2 March 1981 - 1 March 1982

Copy No.

Office of Naval Research
Department of the Navy
Arlington, VA 22217
1 Attn: P. Rogers (Code 425AC)
2 R. Obrochta (Code 230)

Commanding Officer
Naval Ocean Research and Development Activity
NSTL Station, MS 39529
3 Attn: E. D. Chaika (Code 530)
4 W. A. Kuperman (Code 320)
5 CDR M. McCallister (Code 520)

6 Office of Naval Research
Branch Office Chicago
Department of the Navy
536 South Clark Street
Chicago, IL 60605

Commanding Officer
Naval Electronic Systems Command
Washington, DC 20360
7 Attn: LCDR S. Hollis (Code 612)

Commanding Officer
Naval Ocean Systems Center
Department of the Navy
San Diego, CA 92152
8 Attn: E. L. Hamilton
9 H. P. Bucker

Chief of Naval Operations
Department of the Navy
Washington, DC 20350
10 Attn: CAPT J. Harlett (OP 952D)

Distribution List for ARL-TR-82-36, Final Report under Contract N00014-81-K-0353 (Cont'd)

Copy No.

	Chief of Naval Material Department of the Navy Washington, DC 20360
11	Attn: CAPT E. Young (MAT 08T245)
	Director Naval Research Laboratory Department of the Navy Washington, DC 20375
12	Attn: W. B. Moseley (Code 5120)
	Commander Naval Sea Systems Command Department of the Navy Washington, DC 20362
13	Attn: R. W. Farwell (Code 63RA)
14 - 25	Commanding Officer and Director Defense Technical Information Center Cameron Station, Building 5 5010 Duke Street Alexandria, VA 22314
26	Office of Naval Research Resident Representative Room 582, Federal Building Austin, TX 78701
27	Nancy R. Bedford, ARL:UT
28	Glen E. Ellis, ARL:UT
29	Loyd Hampton, ARL:UT
30	Kenneth E. Hawker, ARL:UT
31	Robert A. Koch, ARL:UT
32	Stephen K. Mitchell, ARL:UT
33	Susan G. Payne, ARL:UT
34	Clark S. Penrod, ARL:UT
35	Paul J. Vidmar, ARL:UT
36	Reuben H. Wallace, ARL:UT

Distribution List for ARL-TR-82-36, Final Report under Contract N00014-81-K-0353 (Cont'd)

Copy No.

37	Library, ARL:UT
38 - 48	Reserve, ARL:UT


DATE
ILME